Published in final edited form as:
Cell Rep. 2012 December 27; 2(6): 1593–1606. doi:10.1016/j.celrep.2012.10.016.

Planar Cell Polarity Controls Pancreatic Beta Cell Differentiation and Glucose Homeostasis

Cedric Cortijo[1], **Mathieu Gouzi**[1], **Fadel Tissir**[2], and **Anne Grapin-Botton**[1,3,*]

[1]Swiss Institute for Experimental Cancer Research, Life Sciences, Ecole Polytechnique Fédérale de Lausanne, Station 19, 1015 Lausanne, Switzerland [2]Université Catholique de Louvain, Institute of Neuroscience, Developmental Neurobiology, Avenue E. Mounier, 73, Box B1.73.16, B1200 Brussels, Belgium [3]DanStem, University of Copenhagen, 3B Blegdamsvej, DK-2200 Copenhagen N, Denmark

Summary

Planar cell polarity (PCP) refers to the collective orientation of cells within the epithelial plane. We show that progenitor cells forming the ducts of the embryonic pancreas express PCP proteins and exhibit an active PCP pathway. Planar polarity proteins are acquired at embryonic day 11.5 synchronously to apicobasal polarization of pancreas progenitors. Loss of function of the two PCP core components *Celsr2* and *Celsr3* shows that they control the differentiation of endocrine cells from polarized progenitors, with a prevalent effect on insulin-producing beta cells. This results in a decreased glucose clearance. Loss of *Celsr2* and *3* leads to a reduction of Jun phosphorylation in progenitors, which, in turn, reduces beta cell differentiation from endocrine progenitors. These results highlight the importance of the PCP pathway in cell differentiation in vertebrates. In addition, they reveal that tridimensional organization and collective communication of cells are needed in the pancreatic epithelium in order to generate appropriate numbers of endocrine cells.

Introduction

Polarization of cells in the plane of the epithelium, and perpendicular to the apicobasal axis, is referred to as planar cell polarity (PCP) (Seifert and Mlodzik, 2007) or tissue polarity. PCP mediates cell communication and is important for organized cell movements and morphogenesis of coherently repeated polarized structures such as cilia, hair, or ommatidia. PCP has been well characterized in *Drosophila*, where it was shown that core components display polarized distribution (Bastock et al., 2003; Chen et al., 2008; Gubb and García-Bellido, 1982; Shimada et al., 2001; Strutt and Strutt, 2008, 2009). In many tissues, the Frizzled (FZD), Disheveled (DSH, or DVL in vertebrates) complex is localized at one lateral side of cells, and the strabismus/Van Gogh (STRBM, or VANGL), Prickle (PRK, or PK) complex at the opposite side, whereas Flamingo (FMI, or CELSR 1–3) is symmetrically localized and stabilizes the PCP complexes (Strutt and Strutt, 2008). FMI encodes a protein larger than 3,000 amino acids with N-terminal cadherin repeats, a G-protein-coupled

*Correspondence: anne.grapin-botton@sund.ku.dk.

Supplementary Information: Supplementary Information includes Extended Experimental Procedures and six figures and can be found with this article online at http://dx.doi.org/10.1016/j.celrep.2012.10.016.

receptor proteolysis site (GPS), seven transmembrane domains, and an intracellular C terminus. CELSR1-3 are mammalian homologs of *Drosophila* Flamingo (Usui et al., 1999) and are more than 50% identical in extracellular and transmembrane regions but their cytoplasmic tails differ (Tissir et al., 2005). In *Drosophila*, *Fmi*-null mutations are embryonically lethal as a result of defective longitudinal tracts in the central nervous system (Usui et al., 1999). FMI is implicated, with other PCP pathway components, in the organization of ommatidia, cuticular hairs, wing cells, and sensory bristles in *Drosophila* (Seifert and Mlodzik, 2007). This pathway is highly conserved in vertebrates where it controls neural tube closure (Wang et al., 2006c), convergent extension during gastrulation (Wang et al., 2006a), and hair orientation or sensory cilia orientation in the inner ear (Curtin et al., 2003; Wang et al., 2006b). The conservation of core PCP components and inactivation of PCP genes in different organs shows that the PCP pathway regulates morphogenesis in mammals. For example, in mice, inactivation of *Celsr1* perturbs neural tube closure, but also inner ear cell and skin hair patterning due to a defect of PCP signaling (Curtin et al., 2003; Devenport and Fuchs, 2008; Ravni et al., 2009). *Celsr3* mutation leads to axon tract development defects in the central nervous system and to perturbed facial branchiomotor neuron migration (Qu et al., 2010; Tissir et al., 2005). The *Drosophila* ommatidia are a unique example showing that the PCP can control the specification of cells, namely, photoreceptor R4 (Das et al., 2002).

In this article, we investigated the role of the PCP pathway in pancreas development. The pancreas initially buds from the posterior foregut. From embryonic day 8.5 (E8.5) to E10.5, this bud expands to 500–1,000 multipotent progenitor cells that express PDX1 and SOX9 (Ahlgren et al., 1996; Gu et al., 2002; Lioubinski et al., 2003). At these stages, a few progenitors start to express NEUROG3 and differentiate into endocrine cells, mostly α cells expressing Glucagon (Johansson et al., 2007). Between E11.5 and E14.5, the pancreas progenitors undergo marked remodeling: they become apicobasally polarized and align their apical sides to form ducts (Pan and Wright, 2011). By E14.5, progenitors also become segregated into ductal/endocrine bipotent progenitors in the center of the organ, lining the ducts and exocrine progenitors at terminal end buds (Zhou et al., 2007). At the same time, the progenitors continue to differentiate into endocrine progenitors expressing NEUROG3 and endocrine cells expressing Insulin (β), Somatostatin (δ), Ghrelin (ε), and Pancreatic Polypeptide (PP) and less Glucagon (α) (Johansson et al., 2007). Many transcription factors have been identified that play a role in endocrine cell differentiation (Pan and Wright, 2011). In this study, we investigated the role of cell-cell interactions and how they are constrained by the global architecture of the organ. Recent evidence shows that interfering with the apicobasal polarity of cells has impacts not only on the morphogenesis of the entire organ but also on endocrine differentiation (Kesavan et al., 2009; Villasenor et al., 2010). We therefore investigated whether planar polarity, a pathway that polarizes groups of cells perpendicular to the apicobasal axis, also controls morphogenesis and differentiation.

We show that the core PCP components are expressed during pancreas embryogenesis and are restricted to the epithelium, precisely in pancreas progenitor cells. By deleting *Celsr2* and *Celsr3*, we establish that CELSRs maintain PCP pathway signaling. The disruption of this pathway has little effect on gross acinoductal structure but leads to a severe endocrine cell differentiation defect. Finally, we show that this is caused by modification of JNK signaling in the ducts lined by progenitors.

Results

Planar Polarity Proteins Are Expressed in Pancreas Progenitors Lining Ducts

We initially identified *Celsr3* as a gene that was 8.5-fold upregulated 24 hr after inducing a NEUROG3 gain of function in the pancreatic epithelium at E10.5. In the context of this

profiling experiment using *Pdx1-Ngn3ER-IRES-GFP* mice bred into a *Neurog3*-null background (Gradwohl et al., 2000; Johansson et al., 2007) (data available at http://www.betacell.org), two other Wnt/PCP-related RNAs, *glypican4*, a positive modulator of non-canonical Wnt signaling, and *Dvl1*, were also upregulated (3- and 1.9-fold, respectively). Regulation of *Celsr3* by NEUROG3 was confirmed by quantitative RT-PCR (qRT-PCR) that showed a 50% reduction of *Celsr3* expression in *Neurog3* knockout (KO) at E11.5 (Figure S1A). At E14.5, *Celsr3* expression was no longer modified by *Neurog3* gain or loss of function (data not shown).

To investigate the role of CELSR3 during pancreas development, we analyzed the spatial and temporal expression patterns of *Celsr1–3* transcripts by in situ hybridization (Figures 1A–1H). *Celsr1* and *Celsr3* but not *Celsr2* were detected in the pancreatic bud at E11.5 (Figures 1A–1C). Transcripts for *Celsr1–3* were expressed broadly in the pancreatic epithelium at E14.5 (Figures 1E–1G), including in progenitors, exocrine cells, and endocrine cells (Figures S1F–S1I). Expression was confirmed by qRT-PCR on E14.5 wild-type (WT) pancreas (Figure 4A). To make a more global assessment of the PCP pathway during pancreas development, we first investigated the expression of other core components of the PCP, by RT-PCR, and found that *Prickle1* and *2*, *Vangl1* and *2*, *Dvl1*, *2*, and *3,* and *Fzd3* and *6* are transcribed in the E14.5 pancreas (data not shown).

To gain further insight into the expression and cellular localization of core PCP proteins, we selected VANGL1, which is localized asymmetrically on lateral sides of cells (Wang et al., 2006b). VANGL1 protein becomes consistently detected by E11.5, a stage when apicobasal polarity is first established (Kesavan et al., 2009; Villasenor et al., 2010; Figure 2A). At E11.5 small foci of VANGL1 expression appeared close to the Mucin1 foci marking apical membranes (Figure 2B). At E12.5, the central progenitors expressed membranous VANGL1 but not the tips containing multipotent progenitors (Figures S1B and S1C). After the secondary transition (at E13.5), VANGL1 was detected along the lateral membranes of ductal cells and was apically enriched (Figures 2C, 2D, 2I, and 2J), as reported in other epithelia (Montcouquiol et al., 2006; Shimada et al., 2001; Strutt and Strutt, 2008; Strutt et al., 2011). To determine whether VANGL1 was ubiquitously expressed or restricted to specific cell types, immunostainings against VANGL1 and specific pancreatic markers were performed. We observed that VANGL1 is restricted to $PDX1^+$ and (Figures 2E and 2E′) $SOX9^+$ pancreatic progenitor cells (data not shown), and to $NEUROG3^+$ endocrine progenitors cells (Figures 2F and 2F′). However, no membranous VANGL1 was detected in $Insulin^+$ or $Glucagon^+$ cells (Figures 2G–2H′) or in the acinar compartment at the tip of ducts (Figures 2C, 2E and 2E′, dotted line). VANGL1 is detected in the duct of adult mice (Figures S1D and S1E) even when they have lost progenitor properties (Kopp et al., 2011; Solar et al., 2009).

The Planar Polarity Protein Celsr3 Enables Beta Cell Differentiation

To investigate whether PCP is required for proper pancreas organogenesis, we deleted the PCP core component Celsr3 in mice. Quantification of immunostained sections of *Celsr3* KO mice (Tissir et al., 2005) at E14.5 revealed an increase of the $PDX1^+$ (Figures S2A and S2B) and $SOX9^+$ (data not shown) progenitor cells as well as of the pancreas size. However, this expansion was transient as the size of the pancreas was unaffected at E11.5 and E18.5 (Figures S2C and S2D). Starting from E14.5, we observed a decrease of $Insulin^+$ cells in the KO (Figures 3A–3C), whereas $Glucagon^+$, $Somatostatin^+$, $Ghrelin^+$, and Pancreatic $Polypeptide^+$ cells were unaffected (Figures S2E–S2H). To ascertain that the phenotype observed was due to the function of *Celsr3* in the pancreas epithelium, we specifically inactivated Celsr3 in epithelial pancreas progenitors. We bred *Celsr3 flox/flox* mice (Zhou et al., 2008) with mice expressing a Cre recombinase under the control of the Pdx1 promoter (*Pdx1-Cre*) (Hingorani et al., 2003). In contrast to *Celsr3* KO, *Celsr3 flox/flox; Pdx1-cre*

(abbreviated *Celsr3 f/f; Cre*) did not exhibit the transient increase of pancreatic progenitor cells ($SOX9^+$ cells) (Figure S2I) or of the pancreas size ($Dapi^+$ cells) (Figure S2J), possibly because the *Pdx1-cre*driver leads to delayed or partial recombination. The efficiency of deletion was tested by qRT-PCR at E14.5 and showed a recombination rate of 70% in *Celsr3 f/f; Cre* (Figure S2L). This efficiency is underestimated since an E14.5 pancreas contains about 10% of mesenchyme, which is not targeted by *Pdx1-Cre* (Landsman et al., 2011). As in the KO at E14.5, we observed a reduction of $Insulin^+$ cells (Figure 3D), whereas $Glucagon^+$ cells were unchanged (Figure S2K). Embryos die at P0 after deletion of *Celsr3* most likely due to axonal tract development defects that impair breathing (Tissir et al., 2005), whereas the pancreas specific deletion circumvents the postnatal death. Intraperitoneal glucose tolerance tests on 4-month-old *Celsr3 f/f; Cre* mice revealed a diminished glucose clearance capacity (Figure 3E). Glucose-stimulated insulin secretion (GSIS) in isolated size matched pancreatic islets from 4-month-old mice (Figure 3F) showed that islets from *Celsr3* f/f and *Celsr3* f/f; *Cre* mice did not display any difference in GSIS, indicating that the defect of glucose clearance is not caused by an insulin secretion defect. Thus, we quantified the beta cell population in 4-month-old *Celsr3* f/f and *Celsr3* f/f*; Cre* mice and found that this population was decreased (Figure 3G). Altogether, our findings show that *Celsr3* is needed to generate enough beta cells for appropriate glycemic control.

Celsr2 and *Celsr3* Have Redundant Functions in Pancreas Development and Promote Endocrine Cell Differentiation

It was previously shown that *Celsr2* and *Celsr3* have redundant functions in ependymal cilia development (Tissir et al., 2010) and *Celsr1* and *Celsr2* are also detected in the pancreatic epithelium during development (Figures 1E and 1F). We quantified *Celsr1* and *2* mRNA in *Celsr3* KO mice. *Celsr2* mRNA was significantly increased in *Celsr3* KO pancreatic buds at E14.5 (Figure 4A). Thus, we studied the effect of combined deletion of *Celsr2* and *Celsr3* (DKO) during pancreas development. *Celsr2+3* DKO embryos showed a normal pancreatic progenitor cell population at E14.5 ($SOX9^+$ cells) (Figure S3A) and a normal pancreas size ($Dapi^+$ cells) (Figure S3B). Starting from E14.5, we observed a drastic decrease in $Insulin^+$ cells (Figures 4B–4D) as well as a reduction in all the other endocrine cell populations (Figures 4E-4H). Quantification of the $SOX9^+$, $NEUROG3^+$, $Insulin^+$, $Glucagon^+$ cells, at E14.5 and E18.5 in *Celsr2* mutant mice (Tissir et al., 2010) did not reveal any deviation from WT (Figures S3D–S3F). Thus, Celsr3 is essential for the specification of multipotent progenitors into endocrine cells and Celsr2 substitutes for Celsr3 when the latter is deleted. Beta cells are the most sensitive to the reduction of combined *Celsr* alleles.

Celsr2 and Celsr3 Maintain the PCP in the Pancreas

It was previously shown that disruption of the PCP signaling leads to a positioning defect of PCP proteins to the membrane (Shimada et al., 2001; Tissir et al., 2010). Therefore, to investigate the mechanism of action of *Celsr2+3*, and to assess whether PCP mediates their function, we studied the localization of Vangl1 in *Celsr2+3* DKO pancreas. We observed that VANGL1 was decreased at the membrane of *Celsr3* KO and almost absent in *Celsr2+3* DKO (Figures 5A–5C). We could observe the same reduction of FZD3, another PCP core protein, at the membrane of *Celsr2+3* DKO (Figures S4A and S4B). Furthermore, C-JUN N-terminal kinase (JNK) is activated by PCP signaling in multiple organs (Boutros et al., 1998; Weber et al., 2000; Yamanaka et al., 2002). Therefore, we tested whether JNKactivity was altered in *Celsr3* KO and *Celsr2+3* DKO pancreatic buds by measuring the level of its target phospho-JUN. Consistently, phospho-JUN was downregulated in the mutants as compared with the WT by western blot (Figures 5D–5F). Together, these experiments show that PCP signaling is greatly reduced in *Celsr 2+3* DKO. Although Flamingo, the *Drosophila* Celsr2/3 homolog, is an atypical cadherin that can play a role in adhesion (Usui et al., 1999), E-cadherin (Figures S4C and S4D), ZO-1 immunostainings (data not shown), and electron

microscopy (Figures S4E and S4F) failed to reveal disrupted adherens junctions in *Celsr 2+3* DKO.

Celsr2 and *Celsr3* Control Endocrine Cell Differentiation Downstream of *Neurog3*

To elucidate the mechanism leading to endocrine cell reduction, we first assayed proliferation of beta cells by injecting EdU 1 hr before collecting embryonic pancreata. Quantification of EdU/insulin double-positive cells at the stage of maximal proliferation, in E18.5 embryos, did not reveal differences between *Celsr3* KO, *Celsr2+3* DKO, and WT mice (Figures 5G–5I). Although the proliferation defect may have been earlier, Ki67 immunohistochemistry in WT pancreas at E14.5 revealed a very low proliferation rate of beta cells (2%) and no NEUROG3$^+$ cells were found to be Ki67 positive (data not shown). With this low basal proliferation rate, detecting a decrease of proliferation is rather unlikely. We also quantified the proliferation at E11.5 in WT and *Celsr3* KO and did not detect any difference (data not shown). Apoptosis, monitored by cleaved caspase-3, was minimal at E14.5 and similar between WT and the different *Celsr* mutant mice (data not shown). Thus, these results show that proliferation and apoptosis are unlikely to account for the reduction in endocrine cells. PDX1$^+$ and SOX9$^+$ progenitors give rise to NEUROG3$^+$ cells, which will then differentiate into endocrine cells. Quantification of NEUROG3$^+$ cells did not reveal any difference at E14.5 in WT versus *Celsr3* KO, *Celsr3* f/f; *Cre* or *Celsr2+3* DKO embryos (Figures 5J-5L). However, the number of cells expressing INSM1 and NKX2-2, two transcription factors required for endocrine cell differentiation that are directly induced by NEUROG3 (Gierl et al., 2006; Mellitzer et al., 2006; Smith et al., 2004), was decreased at E14.5 in *Celsr3* f/f; *Cre* and *Celsr2+3* DKO mice (Figures 5M–5O and S3C). These data show that the deletion of *Celsr3* results in a differentiation defect occurring downstream of the NEUROG3$^+$ stage rather than changes in proliferation or apoptosis. The reduction in INSM1-positive cells suggests that NEUROG3$^+$ cells may have a slower differentiation rate or revert to bipotent progenitors. Such reversions have been observed upon reduction of NEUROG3 activity (Magenheim et al., 2011; Wang et al., 2009). Short-term lineage tracing in *Celsr3*$^{-/-}$ *;Neurog3*$^{EYFP/+}$ embryos (Mellitzer et al., 2004), based on the perdurance of YFP signals after NEUROG3 expression did not reveal an increased contribution to the ductal (HNF1B$^+$ and NEUROG3$^-$) or acinar fate (carboxypeptidase A) at E14.5 and E18.5 (data not shown). However, longer-term lineage tracing cumulating the fate of NEUROG3$^+$ cells over time in *Celsr3*$^{-/-}$*; Neurog3-cre; Rosa26-YFP* mice (Schonhoff et al., 2004; Srinivas et al., 2001) revealed a great increase in the contribution to ductal but not to acinar compartment (Figures 6A–6J). The total number of YFP$^+$ cells was similar in both backgrounds, confirming that over time NEUROG3$^+$ cells are generated in normal numbers but are in part rerouted to a ductal fate.

Celsrs Control Beta Cell Differentiation via the Jnk Pathway

JNK mediates some PCP activities in the *Drosophila* eye (Weber et al., 2000) and during convergent extension in *Xenopus* (Yamanaka et al., 2002). Since we observed reduced phospho-JUN upon Celsrs inactivation, the control exerted by Celsrs over endocrine differentiation may be due to impaired JNK activity. JUN is detected by immunohistochemistry in PDX1$^+$ progenitors (Figures 7A and 7A′), in the mesenchyme and is also expressed at lower level in some NEUROG3$^+$ endocrine progenitors cells (Figures 7B and 7B′). However, no JUN is detected in Insulin$^+$ and Glucagon$^+$ cells (Figures 7C and 7C′) or in the acinar compartment (Figures 7D and 7D′). The localization of JUN in the epithelium is thus in the same cell population as the PCP protein VANGL1 (Figures 2E–2H). This global distribution pattern was unaltered in the DKOs although global phospho-JUN levels were decreased. To test whether blocking JNK affects endocrine cell generation, we treated WT pancreatic explants with a specific JNK inhibitor, SP600125 (Bennett et al., 2001), at a time when progenitors start to differentiate into endocrine beta cells (E12.5). We

analyzed the explants treated with SP600125 after culturing for 48 hr (E14.5). We found that inhibiting JNK activity leads to a decrease of the Insulin$^+$ cell number, whereas the PDX1$^+$ cells were unchanged as compared with WT explants treated with the carrier (Figures 7E–7G). The number of Glucagon$^+$ cells was unchanged but a large proportion of these cells were already differentiated at the time of treatment (Johansson et al., 2007). Furthermore, we did not detect any decrease of the NEUROG3$^+$ cells or of the proliferation rate of the total population (Figures S5A and S5B). No Insulin$^+$ cells were found proliferating in explants. Since blocking JUN activity mimics *Celsr3* mutants, we attempted to rescue JNK signaling in *Celsr3 KO*, we treated E12.5 *Celsr3 KO* pancreatic explants with a JNK agonist, anisomycin (Cano et al., 1994). We analyzed the explants treated with anisomycin after culturing for 48 hr (E14.5). A general hypoplasia was measured by a decrease of PDX1 $^+$ cells (Figure 7I). We therefore measured the endocrine differentiation flux by normalizing to the PDX1+ cells and observed a reduction of Insulin$^+$ cells in absolute and relative numbers (Figure 7H). This argues that hyperactive JNK pathway activity limits progenitor expansion and promotes beta cell differentiation.

Discussion

In this study, we have investigated whether the tissue polarity pathway that coordinates individual cell characters in communities of cells impacts the development of the pancreas. Although the role of the PCP in orienting cells has been demonstrated in multiple contexts in vertebrates our experiments reveal that the PCP also controls cell type specification in vertebrates, namely, endocrine cell specification in the pancreas. The only other evidence to our knowledge is the specification of photoreceptors in the *Drosophila* ommatidia (Das et al., 2002).

The PCP Promotes Endocrine Cell Differentiation

We found that constitutive or pancreas-specific deletion of *Celsr3* results in a reduction in Insulin$^+$ cell differentiation and further elimination of Celsr2 alleles potentiates this effect and reduces all other endocrine cell types. Adult mice with a specific deletion of *Celsr3* in PDX1$^+$ pancreatic progenitor cells display glucose intolerance but no functional Insulin secretion defect indicating that CELSRs alter the embryonic endocrine differentiation program and ultimately the number of beta cells in adults. We demonstrate that *Celsrs* are expressed in the pancreas epithelium and control endocrine cell differentiation in this compartment. Moreover, we observe a restriction of VANGL1 and the PCP downstream component cJun to PDX1$^+$/SOX9$^+$ progenitors and NEUROG3$^+$ endocrine progenitors and their decrease upon *Celsr2+3* inactivation. These results suggest that the activity of CELSRs via the PCP in one or both of these progenitor populations leads to reduced endocrine cells. Although the numbersof NEUROG3$^+$ cells was normal in all *Celsr* KOs the reduction of the cells expressing its targets INSM1 and NKX2-2 suggests that their differentiation is arrested after NEUROG3 expression. Lineage tracing shows that a subset of NEUROG3$^+$ cells are rerouted to the ductal compartment, most likely through a bipotent progenitor state. Our interpretation is that the PCP controls either NEUROG3 activity or a NEUROG3 cofactor and that less cells would reach the NEUROG3 threshold to turn on NEUROG3 target genes and further differentiate in the *Celsr* KOs. The induction of this cofactor may occur either in PDX1$^+$/SOX9$^+$ progenitors or in NEUROG3$^+$ progenitors. This is consistent with the observation that similar reversions have been observed with increased frequency upon reduction of NEUROG3 activity (Magenheim et al., 2011; Wang et al., 2009). The reduction of INSM1 and NKX2-2 are consistent with the reduction in endocrine cells but cannot cause the reduced endocrine cell numbers. Indeed, *Insm1* inactivation results in reduced endocrine cell numbers but a large proportion of the cells accumulate in an undifferentiated state (Mellitzer et al., 2006) and *Nkx2-2* deletion results in their conversion to Ghrelin-expressing

cells (Prado et al., 2004), two outcomes that we have not observed in *Celsr* mutants. The minimal proliferation of NEUROG3$^+$ and absence of proliferation of INSM1$^+$ cells we measured in WT makes it unlikely that reduced proliferation at this stage leads to reduced beta cell numbers. Although we did not detect apoptosis, cell death is a fast process and an effect on apoptosis remains possible. Although in the *Drosophila* ommatidia defects in Notch signaling caused by PCP pathway impairments mediated the specification of R3 versus R4 photoreceptors (del Alamo and Mlodzik, 2006; Fanto and Mlodzik, 1999), no changes in the Notch pathway targets *Dll1* or *Hes1* were observed in the pancreas of *Celsr3* and *Celsr2+3* DKO by quantitative RT-PCR.

Upon *Celsr3* inactivation, we did not observe a decrease of the Glucagon$^+$ cells. Our interpretation is that since the PCP is established from E11.5 to E12.5, deletion of Celsrs may only affect late differentiation of endocrine cells. Hence, as a large proportion of Glucagon$^+$ cells are specified between E9.5 and E12.5, unlike other endocrine cell types, they would be less affected. Their decrease may be detected only when the PCP pathway is strongly inactivated as in *Celsr2+3* DKO, thereby making detectable the reduced production of Glucagon cells differentiating after E12.5. This is consistent with the fact that the lineage tracing does not reveal rerouting to the acinar compartment, which we would expect to see if NEUROG3$^+$ cells were converted to the multipotent progenitors residing in the pancreas before E11.5.

Even though endocrine cells are strongly decreased in *Celsr2+3* DKO, their differentiation is not completely impaired. This could be due to a role of the third homolog of Fmi, *Celsr1*, which may substitute for *Celsr2* and *Celsr3* when both are deleted. However no compensatory *Celsr1* upregulation was observed in the *Celsr2+3* KO, and to the contrary, it was reduced by 50% (data not shown). Nevertheless, the persistence of low levels of VANGL1 and FZD3 at the membrane in the *Celsr2+3* DKO suggests that the PCP pathway retains some activity.

The JNK Pathway Regulates Beta Cell Induction Downstream of the PCP

We found that JUN has the same expression pattern as the PCP proteins VANGL1 in progenitor cells but not in endocrine or acinar cells. In agreement with this, we found that deletion of *Celsrs* leads to a decrease of phospho-JUN, suggesting that, as in other systems (Boutros et al., 1998; Weber et al., 2000; Yamanaka et al., 2002), the JNK pathway may mediate at least part of the function of Celsr/PCP complexes in the pancreas (Lapebie et al., 2011). This is a global decrease in each progenitor rather than the disappearance of specific cell types as the global JUN staining pattern remains the same in *Celsrs* KOs. Moreover, JNK pathway inhibition ex vivo impairs Insulin$^+$ cell differentiation, as does the inactivation of *Celsrs*. In addition, the JNK agonist anisomycin applied on pancreatic explants ex vivo resulted in an increased beta cell differentiation flux from progenitors in the *Celsr3* KO, indicating that the JNK pathway promotes beta cell differentiation, and possibly more generally endocrine development. The reduction of phospho-JUN in *Celsr* mutants shows that JUN acts at least in part downstream of *Celsrs*. Hypoplasia was also observed upon JUN overactivation, which could be explained by the fact that overactive JNK triggers endocrine differentiation depleting the pool of progenitors. No defect in adherens junction was detected, thus suggesting that the endocrine cell reduction is not due to adhesion defects either.

Absence of Cysts in PCP-Deficient Mice

In the kidney, strong interferences with the Fat/Dachsous PCP pathway synergizing with *Vangl2*, leads to the formation of ductal enlargements named cysts (Bacallao and McNeill, 2009; Saburi et al., 2008). Impairment of the function of Inversin, a gene that controls

canonical Wnt pathway and planar polarity (Simons et al., 2005) causes cyst formation in the pancreas in addition to the kidney, suggesting a role of PCP in preventing cyst formation in the pancreas. However, no cyst was detected in *Celsr2+3 DKO* or any single mutant in the kidney and pancreas. It is possible that the remaining Celsr1 protein is sufficient to prevent cyst formation or that Celsrs and possibly the PCP pathway do not control ductal diameter in the pancreas. Also, motile cilia formation is impaired in the ependyma of *Celsr2+3* DKO (Tissir et al., 2010). Since cilia defects can cause cysts in the pancreas, we investigated cilia in *Celsr2+3* DKO and found that their structure and occurrence were normal by serial electron microscopy (Figure S6). CELSRs may thus control cilia formation only in some organs or their role may be restricted to motile cilia assembly.

Acquisition of Polarity

VANGL1 starts to be detected at E11.5 in the pancreatic epithelium coinciding with the establishment of apicobasal polarity (Kesavan et al., 2009). Since the PCP factors are apicolaterally localized, the establishment of apicobasal polarity may be a requirement for the establishment of planar polarity and apicobasal determinants may cooperate with PCP factors (Courbard et al., 2009).

Although the PCP proteins were detected at the membrane in the progenitors aligned in the embryonic ducts, it is unclear whether there are two protein complexes restricted to opposing sides of cells as in *Drosophila* or in the mouse inner ear (Seifert and Mlodzik, 2007) or skin (Devenport and Fuchs, 2008). The membranes of two adjacent cells can indeed not be reliably discriminated with conventional microscopy. How an asymmetry in expression may control differentiation remains to be elucidated even if asymmetric cell division or asymmetric repartition of key receptors for privileged reception of a ligand may be invoked.

In vitro differentiation of beta cells from ES cells, for the purpose of cell therapy of diabetes, has greatly progressed in the past years but the final step of production of endocrine cells from pancreas progenitors is ineffective in 2D cultures, although the progenitors reveal their potential to differentiate into beta cells when transplanted in vivo (Kroon et al., 2008). Previous work has shown that proper apicobasal polarity is required for beta cell production in vivo and our experiments demonstrate that PCP also promotes endocrine differentiation. The implementation of culture conditions with controlled polarization in 3D may thus help promote the differentiation of beta cells in vitro.

Experimental Procedures

In Situ Hybridization

In situ hybridization was conducted as described previously (Gouzi et al., 2011). Probes are specified in Supplemental Information.

Immunofluorescence

Mouse embryos were fixed in 4% paraformaldehyde for 30 min to 1 hr at room temperature or overnight at 4°C. After several washes in 1 × PBS, embryos were equilibrated in 15% sucrose (Applichem) in Phosphate Buffer 0.12 M prior to embedding in 7.5% gelatin (Sigma), 15% sucrose in phosphate buffer 0.12 M. Gelatin blocks were subsequently frozen in −65°C 2-methylbutane (isopentane, Acros Organics) and kept at −80°C until sectioning. Frozen sections (8 μm) were then dried at room temperature and washed in 1 × PBS, before 30 min blocking in 1% BSA. Primary antibodies were incubated overnight at 4°C. A primary antibody list is provided in Supplemental Information. Secondary antibodies were incubated 1 hr at room temperature. Alexa Fluor secondary antibodies (all from Molecular

Probes-Invitrogen) were used for multicolor detection. Nuclei were stained with DAPI (50 ng/μl; Sigma). The sections were mounted in 50% PBS:50% glycerol with a coverslip covering the entire surface of the slide. All fluorescence microscopy images were taken with a Leica DM5500 or a Zeiss LSM700 confocal microscope.

Immunoblotting

Mice were killed and pancreatic buds were taken and frozen in liquid nitrogen. Pancreas were disrupted mechanically and sonicated. Antibodies against phospho-JUN^{Ser73} (cell signaling) and gamma-tubulin (Sigma) were used.

Electron Microscopy

Pancreata were fixed by perfusion with 5% glutaraldehyde and 2% paraformaldehyde in 0.1 M PBS (pH 7.4) and were postfixed for 1 hr in 1% osmium tetroxide and 1.5% potassium ferrocyanide in cacodylate buffer (0.1 M, pH 7.4). Thin serial sections were stained with uranyl acetate and lead citrate, and observed with a FEI Tecnai Spirit 120 kV transmission electron microscope.

Mouse Strains

Mouse lines we used were previously described and are referenced in the result section. The Swiss Veterinary Office approved all animal experiments. Embryos were collected at indicated times; midday on the day of vaginal plug appearance was considered E0.5. The *Tg(Neurog3-cre)C1Able and Gt(ROSA)26Sor$^{tm1(EYFP)Cos}$* lines are respectively simplified as *Neurog3-Cre* and *Rosa26-YFP* in the results.

Genotyping

For genotyping, biopsies or embryonic mouse tissue collected during dissection were digested in 100–200 μl of DirectPCR tail buffer (Viagen-Biotech) with 2.5 μl of Proteinase K recombinant PCR grade (Roche Applied Sciences) in a heating block at 55°C overnight. Proteinase K was inactivated at 85°C during 45 min. PCR was run using 2 μl of lysate and the primers described in the respective references.

Quantification and Statistical Analysis

For quantification, the entire pancreas was serially sectioned. The total number of cells per pancreas was obtained by counting immunopositive cells on every 6th (E14.5), 8th (E18.5), or 20th section (4 months). For explants, sections were collected in four consecutive series. For NEUROG3, INSM1, NKX2-2, Ghrelin, Somatostatin, and Pancreatic Polypeptide positive cells (matching a Dapi^{+} nucleus) were counted manually. For Insulin, Glucagon, PDX1, SOX9, and Dapi, the positive pixels (surface of section) were quantified. All values are shown as mean ± SD with *n* numbers and internal replicates indicated in the figure of the legend; p values were calculated using the nonparametric unpaired Mann-Whitney test unless otherwise indicated; $p < 0.05$ was considered significant.

Quantitative Real-Time PCR

Methods and primers are provided in the Extended Experimental Procedures.

Glucose Tolerance Test

For glucose tolerance tests, blood samples were obtained from the tail vein of overnight-fasted mice to measure glucose levels using a freestyle pen (Abbott, USA). Samples were measured immediately before and 15, 30, 45, 60, and 90 min after intraperitoneal injection of 2 g/kg glucose.

Insulin Secretion

Pancreatic islets were isolated via bile duct collagenase digestion (Collagenase P, Roche) left to recover overnight at 37°C in RPMI 1640 with 10% FBS, 1% L-glutamineand 1% penicillin/streptomycin. For insulin release assays, 15 islets of matched size were statically incubated in Krebs-Ringer Buffer and stimulated for 30 min at 37°C with various glucose concentrations, 2.8 or 15 mM. Supernatant was collected and assayed for insulin content by ELISA. Islets were then sonicated in acid-ethanol solution and solubilized overnight at 4°C before assaying total insulin content by ELISA.

Culture of Pancreatic Explants

E12.5 dorsal pancreatic buds were dissected and cultured on Millipore filters for 2 days in culture medium (BioWhittaker Medium 199,10% fetal calf serum, 1% penicillin-streptomycin) in the presence or absence of 10 μM JNK inhibitor, SP600125 (Calbiochem) or 50 ng/ml JNK agonist, anisomycin (Sigma). The culture medium was changed every day and, by the end of the culture period, explants were embedded in gelatin and processed as described above for immunostaining analysis.

Supplementary Material

Refer to Web version on PubMed Central for supplementary material.

Acknowledgments

This work was supported by a Swiss National Science Foundation grant 31003A-127071 to A.G.-B. and NIDDK 1U01DK089570-01, as part of the Beta Cell Biology Consortium. M.G. identified *Celsr3* as a NEUROG3 target. C.C. performed all other experiments. F.T. generated *Celsr2* and *3* targeted mice. C.C. and A.G.-B. wrote the manuscript and F.T. and M.G. commented on it. We thank Jeremy Nathans and Gérard Gradwohl for generously sharing the FZD3 and INSM1 antibodies. We would like to thank C. Greggio, D. Martin, L. Flasse, and M.R.-C. Kraus for their experimental help. We are grateful to J. Brickman and A. Martinez-Arias for their comments on the manuscript.

References

Ahlgren U, Jonsson J, Edlund H. The morphogenesis of the pancreatic mesenchyme is uncoupled from that of the pancreatic epithelium in IPF1/PDX1 -deficient mice. Development. 1996; 122:1409–1416. [PubMed: 8625829]

Bacallao RL, McNeill H. Cystic kidney diseases and planar cell polarity signaling. Clin Genet. 2009; 75:107–117. [PubMed: 19215242]

Bastock R, Strutt H, Strutt D. Strabismus is asymmetrically localised and binds to Prickle and Dishevelled during Drosophila planar polarity patterning. Development. 2003; 130:3007–3014. [PubMed: 12756182]

Bennett BL, Sasaki DT, Murray BW, O'Leary EC, Sakata ST, Xu W, Leisten JC, Motiwala A, Pierce S, Satoh Y, et al. SP600125, an anthrapyrazolone inhibitor of Jun N-terminal kinase. Proc Natl Acad Sci USA. 2001; 98:13681–13686. [PubMed: 11717429]

Boutros M, Paricio N, Strutt DI, Mlodzik M. Dishevelled activates JNK and discriminates between JNK pathways in planar polarity and wingless signaling. Cell. 1998; 94:109–118. [PubMed: 9674432]

Cano E, Hazzalin CA, Mahadevan LC. Anisomycin-activated protein kinases p45 and p55 but not mitogen-activated protein kinases ERK-1 and -2 are implicated in the induction of c-fos and c-jun. Mol Cell Biol. 1994; 14:7352–7362. [PubMed: 7935449]

Chen WS, Antic D, Matis M, Logan CY, Povelones M, Anderson GA, Nusse R, Axelrod JD. Asymmetric homotypic interactions of the atypical cadherin flamingo mediate intercellular polarity signaling. Cell. 2008; 133:1093–1105. [PubMed: 18555784]

Courbard JR, Djiane A, Wu J, Mlodzik M. The apical/basal-polarity determinant Scribble cooperates with the PCP core factor Stbm/Vang and functions as one of its effectors. Dev Biol. 2009; 333:67–77. [PubMed: 19563796]

Curtin JA, Quint E, Tsipouri V, Arkell RM, Cattanach B, Copp AJ, Henderson DJ, Spurr N, Stanier P, Fisher EM, et al. Mutation of Celsr1 disrupts planar polarity of inner ear hair cells and causes severe neural tube defects in the mouse. Curr Biol. 2003; 13:1129–1133. [PubMed: 12842012]

Das G, Reynolds-Kenneally J, Mlodzik M. The atypical cadherin Flamingo links Frizzled and Notch signaling in planar polarity establishment in the Drosophila eye. Dev Cell. 2002; 2:655–666. [PubMed: 12015972]

del Alamo D, Mlodzik M. Frizzled/PCP-dependent asymmetric neuralized expression determines R3/R4 fates in the Drosophila eye. Dev Cell. 2006; 11:887–894. [PubMed: 17141162]

Devenport D, Fuchs E. Planar polarization in embryonic epidermis orchestrates global asymmetric morphogenesis of hair follicles. Nat Cell Biol. 2008; 10:1257–1268. [PubMed: 18849982]

Fanto M, Mlodzik M. Asymmetric Notch activation specifies photoreceptors R3 and R4 and planar polarity in the Drosophila eye. Nature. 1999; 397:523–526. [PubMed: 10028968]

Gierl MS, Karoulias N, Wende H, Strehle M, Birchmeier C. The zinc-finger factor Insm1 (IA-1) is essential for the development of pancreatic beta cells and intestinal endocrine cells. Genes Dev. 2006; 20:2465–2478. [PubMed: 16951258]

Gouzi M, Kim YH, Katsumoto K, Johansson K, Grapin-Botton A. Neurogenin3 initiates stepwise delamination of differentiating endocrine cells during pancreas development. Dev Dyn. 2011; 240:589–604. [PubMed: 21287656]

Gradwohl G, Dierich A, LeMeur M, Guillemot F. neurogenin3 is required for the development of the four endocrine cell lineages of the pancreas. Proc Natl Acad Sci USA. 2000; 97:1607–1611. [PubMed: 10677506]

Gu G, Dubauskaite J, Melton DA. Direct evidence for the pancreatic lineage: NGN3+ cells are islet progenitors and are distinct from duct progenitors. Development. 2002; 129:2447–2457. [PubMed: 11973276]

Gubb D, García-Bellido A. A genetic analysis of the determination of cuticular polarity during development in Drosophila melanogaster. J Embryol Exp Morphol. 1982; 68:37–57. [PubMed: 6809878]

Hingorani SR, Petricoin EF, Maitra A, Rajapakse V, King C, Jacobetz MA, Ross S, Conrads TP, Veenstra TD, Hitt BA, et al. Preinvasive and invasive ductal pancreatic cancer and its early detection in the mouse. Cancer Cell. 2003; 4:437–450. [PubMed: 14706336]

Johansson KA, Dursun U, Jordan N, Gu G, Beermann F, Gradwohl G, Grapin-Botton A. Temporal control of neurogenin3 activity in pancreas progenitors reveals competence windows for the generation of different endocrine cell types. Dev Cell. 2007; 12:457–465. [PubMed: 17336910]

Kesavan G, Sand FW, Greiner TU, Johansson JK, Kobberup S, Wu X, Brakebusch C, Semb H. Cdc42-mediated tubulogenesis controls cell specification. Cell. 2009; 139:791–801. [PubMed: 19914171]

Kopp JL, Dubois CL, Schaffer AE, Hao E, Shih HP, Seymour PA, Ma J, Sander M. Sox9+ ductal cells are multipotent progenitors throughout development but do not produce new endocrine cells in the normal or injured adult pancreas. Development. 2011; 138:653–665. [PubMed: 21266405]

Kroon E, Martinson LA, Kadoya K, Bang AG, Kelly OG, Eliazer S, Young H, Richardson M, Smart NG, Cunningham J, et al. Pancreatic endoderm derived from human embryonic stem cells generates glucose-responsive insulin-secreting cells in vivo. Nat Biotechnol. 2008; 26:443–452. [PubMed: 18288110]

Landsman L, Nijagal A, Whitchurch TJ, Vanderlaan RL, Zimmer WE, Mackenzie TC, Hebrok M. Pancreatic mesenchyme regulates epithelial organogenesis throughout development. PLoS Biol. 2011; 9:e1001143. [PubMed: 21909240]

Lapebie P, Borchiellini C, Houliston E. Dissecting the PCP pathway: one or more pathways?: Does a separate Wnt-Fz-Rho pathway drive morphogenesis? BioEssays. 2011; 33:759–768. [PubMed: 21919026]

Lioubinski O, Müller M, Wegner M, Sander M. Expression of Sox transcription factors in the developing mouse pancreas. Dev Dyn. 2003; 227:402–408. [PubMed: 12815626]

Magenheim J, Klein AM, Stanger BZ, Ashery-Padan R, Sosa-Pineda B, Gu G, Dor Y. Ngn3(+) endocrine progenitor cells control the fate and morphogenesis of pancreatic ductal epithelium. Dev Biol. 2011; 359:26–36. [PubMed: 21888903]

Mellitzer G, Martín M, Sidhoum-Jenny M, Orvain C, Barths J, Seymour PA, Sander M, Gradwohl G. Pancreatic islet progenitor cells in neurogenin 3-yellow fluorescent protein knock-add-on mice. Mol Endocrinol. 2004; 18:2765–2776. [PubMed: 15297605]

Mellitzer G, Bonné S, Luco RF, Van De Casteele M, Lenne-Samuel N, Collombat P, Mansouri A, Lee J, Lan M, Pipeleers D, et al. IA1 is NGN3-dependent and essential for differentiation of the endocrine pancreas. EMBO J. 2006; 25:1344–1352. [PubMed: 16511571]

Montcouquiol M, Sans N, Huss D, Kach J, Dickman JD, Forge A, Rachel RA, Copeland NG, Jenkins NA, Bogani D, et al. Asymmetric localization of Vangl2 and Fz3 indicate novel mechanisms for planar cell polarity in mammals. J Neurosci. 2006; 26:5265–5275. [PubMed: 16687519]

Pan FC, Wright C. Pancreas organogenesis: from bud to plexus to gland. Dev Dyn. 2011; 240:530–565. [PubMed: 21337462]

Prado CL, Pugh-Bernard AE, Elghazi L, Sosa-Pineda B, Sussel L. Ghrelin cells replace insulin-producing beta cells in two mouse models of pancreas development. Proc Natl Acad Sci USA. 2004; 101:2924–2929. [PubMed: 14970313]

Qu Y, Glasco DM, Zhou L, Sawant A, Ravni A, Fritzsch B, Damrau C, Murdoch JN, Evans S, Pfaff SL, et al. Atypical cadherins Celsr1-3 differentially regulate migration of facial branchiomotor neurons in mice. J Neurosci. 2010; 30:9392–9401. [PubMed: 20631168]

Ravni A, Qu Y, Goffinet AM, Tissir F. Planar cell polarity cadherin Celsr1 regulates skin hair patterning in the mouse. J Invest Dermatol. 2009; 129:2507–2509. [PubMed: 19357712]

Saburi S, Hester I, Fischer E, Pontoglio M, Eremina V, Gessler M, Quaggin SE, Harrison R, Mount R, McNeill H. Loss of Fat4 disrupts PCP signaling and oriented cell division and leads to cystic kidney disease. Nat Genet. 2008; 40:1010–1015. [PubMed: 18604206]

Schonhoff SE, Giel-Moloney M, Leiter AB. Neurogenin 3-expressing progenitor cells in the gastrointestinal tract differentiate into both endocrine and non-endocrine cell types. Dev Biol. 2004; 270:443–454. [PubMed: 15183725]

Seifert JRK, Mlodzik M. Frizzled/PCP signalling: a conserved mechanism regulating cell polarity and directed motility. Nat Rev Genet. 2007; 8:126–138. [PubMed: 17230199]

Shimada Y, Usui T, Yanagawa S, Takeichi M, Uemura T. Asymmetric colocalization of Flamingo, a seven-pass transmembrane cadherin, and Dishevelled in planar cell polarization. Curr Biol. 2001; 11:859–863. [PubMed: 11516647]

Simons M, Gloy J, Ganner A, Bullerkotte A, Bashkurov M, KrÖnig C, Schermer B, Benzing T, Cabello OA, Jenny A, et al. Inversin, the gene product mutated in nephronophthisis type II, functions as a molecular switch between Wnt signaling pathways. Nat Genet. 2005; 37:537–543. [PubMed: 15852005]

Smith SB, Watada H, German MS. Neurogenin3 activates the islet differentiation program while repressing its own expression. Mol Endocrinol. 2004; 18:142–149. [PubMed: 14576336]

Solar M, Cardalda C, Houbracken I, Martín M, Maestro MA, De Medts N, Xu X, Grau V, Heimberg H, Bouwens L, Ferrer J. Pancreatic exocrine duct cells give rise to insulin-producing beta cells during embryogenesis but not after birth. Dev Cell. 2009; 17:849–860. [PubMed: 20059954]

Srinivas S, Watanabe T, Lin CS, William CM, Tanabe Y, Jessell TM, Costantini F. Cre reporter strains produced by targeted insertion of EYFP and ECFP into the ROSA26 locus. BMC Dev Biol. 2001; 1:4. [PubMed: 11299042]

Strutt H, Strutt D. Differential stability of flamingo protein complexes underlies the establishment of planar polarity. Curr Biol. 2008; 18:1555–1564. [PubMed: 18804371]

Strutt H, Strutt D. Asymmetric localisation of planar polarity proteins: Mechanisms and consequences. Semin Cell Dev Biol. 2009; 20:957–963. [PubMed: 19751618]

Strutt H, Warrington SJ, Strutt D. Dynamics of core planar polarity protein turnover and stable assembly into discrete membrane subdomains. Dev Cell. 2011; 20:511–525. [PubMed: 21497763]

Tissir F, Bar I, Jossin Y, De Backer O, Goffinet AM. Protocadherin Celsr3 is crucial in axonal tract development. Nat Neurosci. 2005; 8:451–457. [PubMed: 15778712]

Tissir F, Qu Y, Montcouquiol M, Zhou L, Komatsu K, Shi D, Fujimori T, Labeau J, Tyteca D, Courtoy P, et al. Lack of cadherins Celsr2 and Celsr3 impairs ependymal ciliogenesis, leading to fatal hydrocephalus. Nat Neurosci. 2010; 13:700–707. [PubMed: 20473291]

Usui T, Shima Y, Shimada Y, Hirano S, Burgess RW, Schwarz TL, Takeichi M, Uemura T. Flamingo, a seven-pass transmembrane cadherin, regulates planar cell polarity under the control of Frizzled. Cell. 1999; 98:585–595. [PubMed: 10490098]

Villasenor A, Chong DC, Henkemeyer M, Cleaver O. Epithelial dynamics of pancreatic branching morphogenesis. Development. 2010; 137:4295–4305. [PubMed: 21098570]

Wang J, Hamblet NS, Mark S, Dickinson ME, Brinkman BC, Segil N, Fraser SE, Chen P, Wallingford JB, Wynshaw-Boris A. Dishevelled genes mediate a conserved mammalian PCP pathway to regulate convergent extension during neurulation. Development. 2006a; 133:1767–1778. [PubMed: 16571627]

Wang Y, Guo N, Nathans J. The role of Frizzled3 and Frizzled6 in neural tube closure and in the planar polarity of inner-ear sensory hair cells. J Neurosci. 2006b; 26:2147–2156. [PubMed: 16495441]

Wang Y, Guo N, Nathans J. The role of Frizzled3 and Frizzled6 in neural tube closure and in the planar polarity of inner-ear sensory hair cells. J Neurosci. 2006c; 26:2147–2156. [PubMed: 16495441]

Wang S, Jensen JN, Seymour PA, Hsu W, Dor Y, Sander M, Magnuson MA, Serup P, Gu G. Sustained Neurog3 expression in hormone-expressing islet cells is required for endocrine maturation and function. Proc Natl Acad Sci USA. 2009; 106:9715–9720. [PubMed: 19487660]

Weber U, Paricio N, Mlodzik M. Jun mediates Frizzled-induced R3/R4 cell fate distinction and planar polarity determination in the Drosophila eye. Development. 2000; 127:3619–3629. [PubMed: 10903185]

Yamanaka H, Moriguchi T, Masuyama N, Kusakabe M, Hanafusa H, Takada R, Takada S, Nishida E. JNK functions in the non-canonical Wnt pathway to regulate convergent extension movements in vertebrates. EMBO Rep. 2002; 3:69–75. [PubMed: 11751577]

Zhou L, Bar I, Achouri Y, Campbell K, De Backer O, Hebert JM, Jones K, Kessaris N, de Rouvroit CL, O'Leary D, et al. Early forebrain wiring: genetic dissection using conditional Celsr3 mutant mice. Science. 2008; 320:946–949. [PubMed: 18487195]

Zhou Q, Law AC, Rajagopal J, Anderson WJ, Gray PA, Melton DA. A multipotent progenitor domain guides pancreatic organogenesis. Dev Cell. 2007; 13:103–114. [PubMed: 17609113]

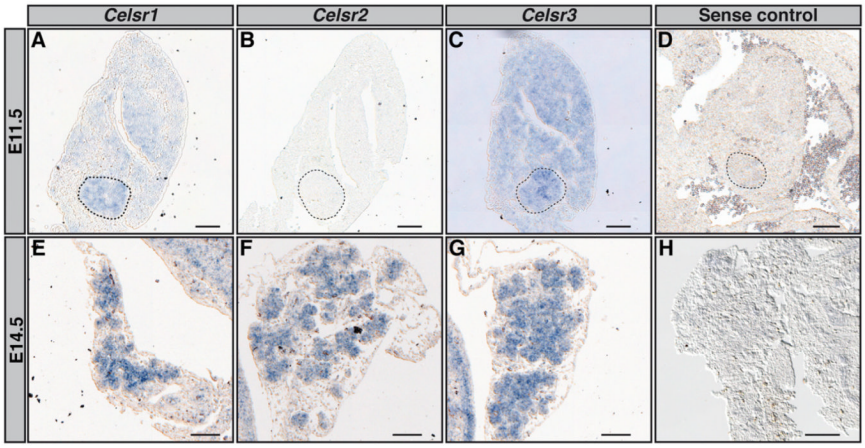

Figure 1. *Celsr1, Celsr2,* and *Celsr3* Are Expressed in the Epithelium of the Pancreas

(A–H) In situ hybridization detecting *Celsr1–3* mRNA expression was performed on 8 μm sections at E11.5 (A–C) and E14.5 (E–G). *Celsr1* (A) and *Celsr3* (C) are detected at E11.5, but not *Celsr2* (B). *Celsr1* (E), *Celsr*2 (F), and *Celsr3* (G) are expressed in the pancreatic epithelium at E14.5. Sense probes for *Celsr1–3* exhibited no staining as shown for *Celsr3* (D and H). (A–D) Dotted lines show the pancreatic bud. Scale bars, 25 μm (A–D) and 100 μm (E–H), n = 4.

See also Figure S1.

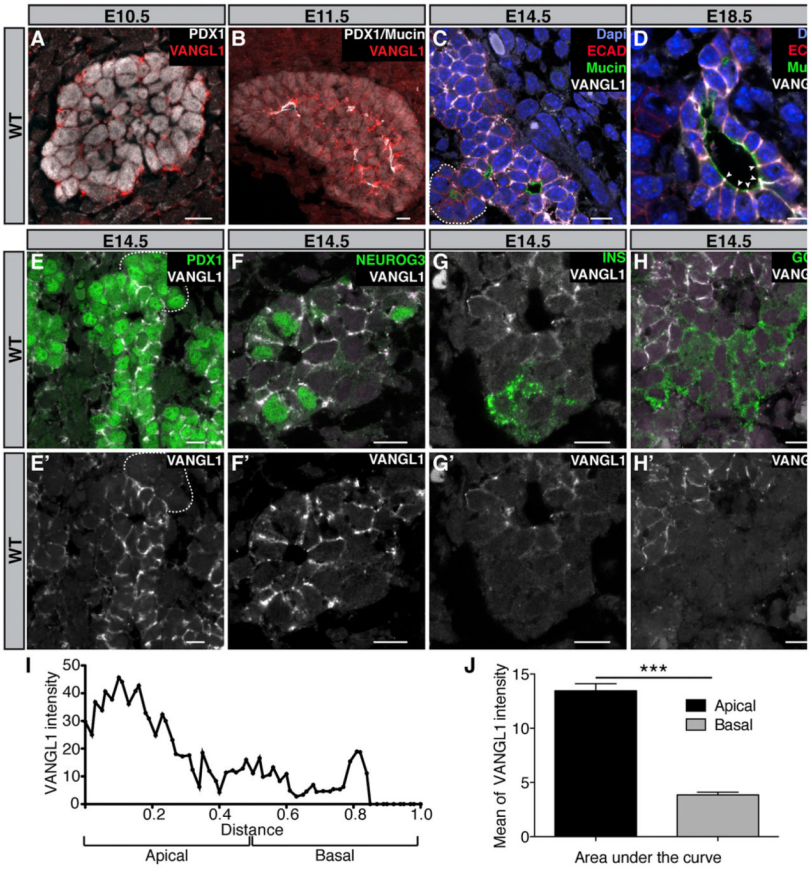

Figure 2. The Planar Cell Polarity Protein VANGL1 Is Restricted to Progenitor Cells

Representative sections of E10.5–E18.5 WT pancreata immunostained against the indicated antigens (A–H).

(A) E10.5 pancreas section immunostained with antibodies against PDX1 (white), pancreatic progenitor marker, and VANGL1 (red). No reproducible VANGL1 signal is detected, only random background.

(B) E11.5 pancreas section immunostained with antibodies against PDX1, Mucin1 (white), apical marker, and VANGL1 (red). VANGL1 is enriched close to the apical surface of cells.

(C and D) E14.5–E18.5 pancreas sections stained with Dapi (blue) and antibodies against ECAD (red), epithelial marker, Mucin1 (green), and VANGL1 (white). VANGL1 is expressed in the ductal compartment but not in the exocrine compartment delimited by the dotted line, preferentially at the apicolateral surface of cells (arrowhead).

(E–H) E14.5 pancreas sections immunostained with antibodies against PDX1, NEUROG3, endocrine progenitor marker, Insulin (INS) or Glucagon (GCG) (green), and VANGL1 (white). $PDX1^+$ and $NEUROG3^+$ cells are $VANGL1^+$, whereas INS^+, GCG^+ cells and the acinar compartment (dotted line) are $VANGL1^-$. (E′–H′) Only VANGL1 (white) is shown. Scale bars, 10 μm.

(I) Localization of VANGL1 along the lateral membrane of cells. Measurement of VANGL1 intensity signal at E18.5 along the apicobasal axis of the membrane shows apredominant expression at the apicolateral side of the cell (n = 31). The limit between apical and basal side of the membrane is positioned at the middle of the absolute length of the membrane. The distance from the apical (Mucin1) to the basal (mesenchyme) is set to normalize between the different cells.

(J) Area under the curve of apical VANGL1 versus basal VANGL1 intensity (n = 31).

***p < 0.0001. Bars show SDs and p values are calculated according to Mann-Whitney U test.

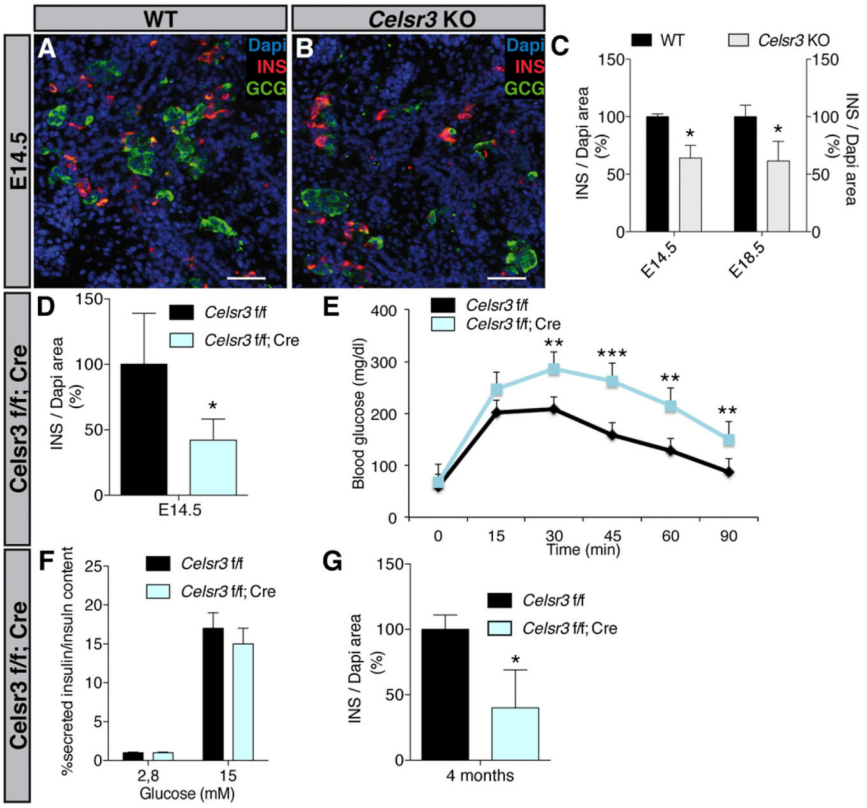

Figure 3. *Celsr3* Deletion Results in Decreased β Cell Population and Glucose Intolerance

(A and B) E14.5 WT and *Celsr3* KO serial pancreas sections were stained with Dapi (blue), and antibodies against Insulin (INS; red) and Glucagon (GCG; green). Scale bar, 50 μm.

(C and D) INS/Dapi area was quantified at E14.5 and E18.5. In *Celsr3* KO embryos, INS area is significantly reduced compared to WT (n = 4), *p < 0.05. (D) E14.5 *Celsr3* f/f and *Celsr3* f/f; Cre were stained with Dapi (blue) and an antibody against Insulin. INS/Dapi area was quantified at E14.5. In *Celsr3* f/f; Cre embryos, INS area is significantly decreased compared to WT (n = 4), *p < 0.05.

(E) Intraperitoneal glucose tolerance tests were performed on 4-month-old *Celsr3* f/f and *Celsr3* f/f; Cre mice, fasted for 16 hr. Glucose (2 g/kg) was administered at time 0. Each point represents the mean of nine mice. Basal fasting blood glucose levels are similar between the two groups of mice. The *Celsr3* f/f; Cre mice exhibit significantly higher blood glucose levels. (n = 9), **p < 0.001, ***p < 0.0001.

(F) Insulin secretion normalized to total Insulin content in *Celsr3* f/f and *Celsr3* f/f; Cre islets at the indicated glucose concentrations (n = 4 mice for each genotype). No differences are observed.

(G) INS/Dapi area was quantified at 4 months. In *Celsr3* f/f*; Cre* adults, INS area is significantly decreased compared to WT (n = 4), *p < 0.05. Bars show SDs and p values are calculated according to Mann-Whitney U test.

See also Figure S2.

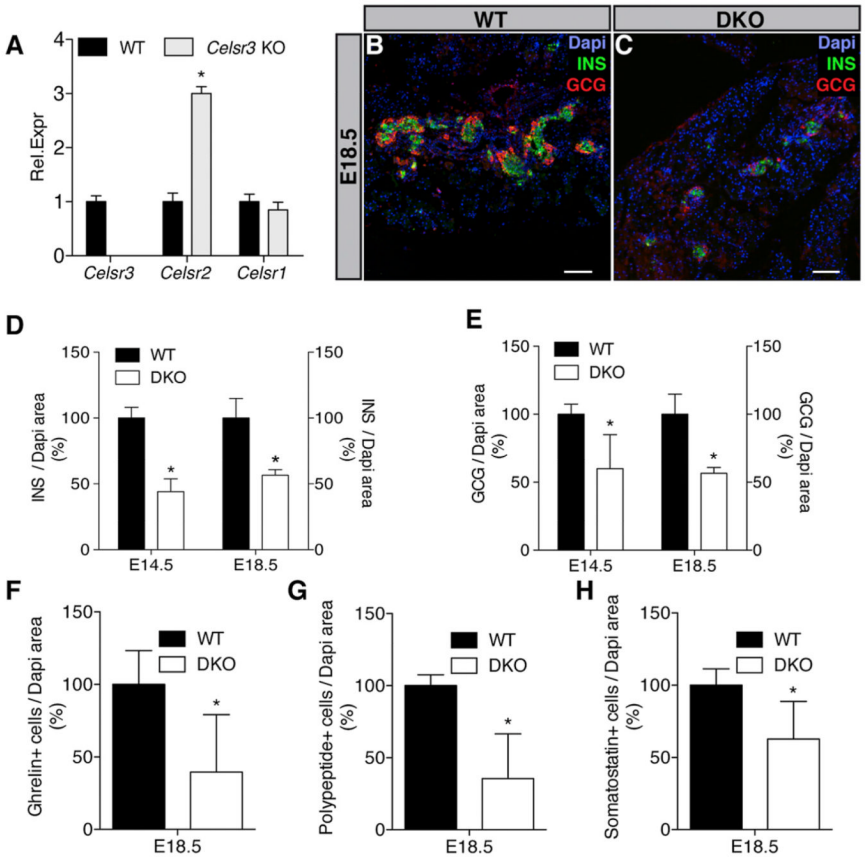

Figure 4. Celsr3 and Celsr2 Promote Endocrine Cell Differentiation

(A) qRT-PCR analysis on E14.5 WT and *Celsr3* KO embryos shows an increase in the relative expression of *Celsr2* (n = 4), *p < 0.05.

(B and C) Serial pancreas sections from E18.5 WT and *Celsr2+3* DKO embryos (DKO) were stained with Dapi (blue) and antibodies against INS (red) and GCG (green). Scale bar, 100 μm.

(D) At E14.5 and E18.5, INS/Dapi area was quantified. In DKO embryos, INS area is decreased compared to WT (n = 4), *p < 0.05.

(E) At E14.5 and E18.5, GCG/Dapi area was quantified. In DKO embryos, GCG area is decreased compared to WT (n = 4), *p < 0.05.

(F–H) The Ghrelin$^+$, Pancreatic Polypeptide$^+$, and Somatostatin$^+$ cells were quantified at E18.5. In DKO embryos, Ghrelin$^+$, Pancreatic Polypeptide$^+$, and Somatostatin$^+$ cells are decreased compared to WT (n = 4), *p < 0.05.

Bars show SDs and p values are calculated according to Mann-Whitney U test. See also Figure S3.

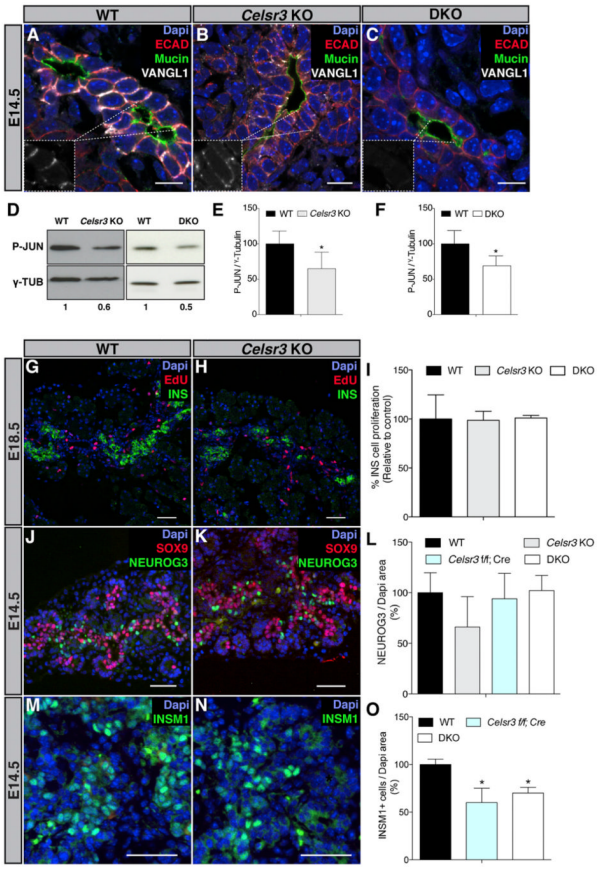

Figure 5. CELSR2+3 Function via PCP Signaling and Control Endocrine Differentiation Downstream of NEUROG3

(A–C) E14.5 WT, *Celsr3* KO, and *Celsr2+3* DKO serial pancreas sections were stained with Dapi (blue), and antibodies against ECAD (red), epithelial marker, Mucin1 (green), and VANGL1 (white). Scale bar, 50 μm. VANGL1 is reduced at the plasma membrane of *Celsr3* KO and almost absent in *Celsr2+3* DKO (n = 4).

(D) Western blot against phospho-JUN. *Celsr3* and *Celsr2+3* deletion resulted in lower PCP signaling level (n = 3 independent experiments, each on three pooled E14.5 pancreas per lane).

(E and F) Mean of the quantification of the band intensity for *Celsr3* KO and *Celsr2+3* DKO (n = 3). *p < 0.05. Bars show SDs and p values are calculated according to t test, hypothesizing a standard normal distribution.

(G and H) Serial pancreas sections of E14.5 WT and *Celsr3* KO were stained with Dapi (blue) EdU (red), proliferation marker, and INS (green). Scale bar, 50 μm.

(I) The percentage of Insulin^{+} cells that costained with EdU is not different between WT, *Celsr3* KO, and *Celsr 2+3* DKO embryos (n = 4).

(J and K) Serial pancreas sections of E14.5 WT and *Celsr3* KO were stained with Dapi (blue) and antibodies against SOX9 (red) and NEUROG3 (green). Scale bar, 50 μm.

(L) Quantification of the number of NEUROG3^{+} cells in WT, *Celsr3* KO, *Celsr3 f/f; Cre*, and *Celsr 2+3* DKO embryos did not show any difference (n = 4).

(M and N) Serial pancreas sections of E14.5 WT and *Celsr3* KO embryos were stained with Dapi (blue) and antibodies against INSM1 (green). Scale bar, 50 μm.

(O) Quantification of INSM1^{+} cells shows a significant decrease in *Celsr3 f/f; Cre* and *Celsr2+3* DKO compared to the WT. (n = 4), *p < 0.05.

Bars show SDs and p values are calculated according to the Mann-Whitney U test. See also Figures S4 and S6.

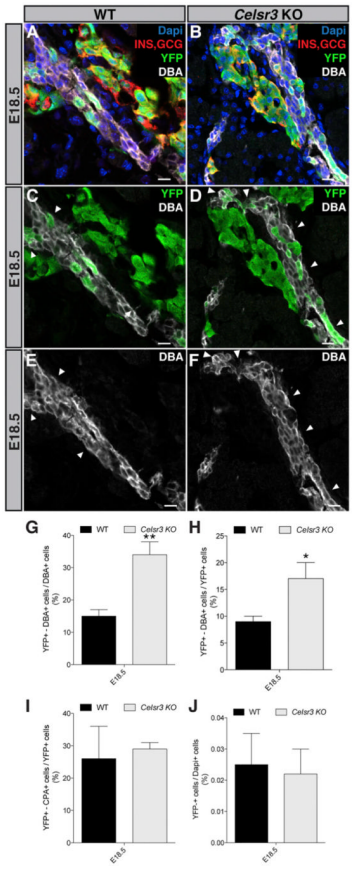

Figure 6. Fate of Endocrine Progenitor Cells in *Celsr3* KO Pancreas

(A–F) E18.5 *Neurog3-Cre; Rosa26-YFP* mice harboring WT or *Celsr3* KO alleles immunostained with antibodies against DBA-lectin, ductal marker (white), YFP (green), and Insulin/Glucagon, endocrine marker (red). Arrowheads show YFP^+ cells that are DBA^+.

(G) Number of cells that are YFP^+ and DBA^+, normalizedon the total DBA^+ cells in pancreas. In *Celsr3* KO embryos we observed that 35% progeny of NEUROG3-expressing cells remain confined within the DBA^+ epithelium cells compared to 15% in the WT (n = 3).

(H) Number of cells that are YFP^+ and DBA^+, normalized to the total YFP^+ cells in pancreas (n = 3).

(I) Number of cells that are YFP^+ and CPA^+, normalized to the total YFP^+ cells in pancreas (n = 3).

(J) Number of cells that are YFP^+, normalized to the total $Dapi^+$ cells in pancreas (n = 3). No difference was observed. Scale bar, 10 μm.

Bars show SDs and p values are calculated according to the t test.

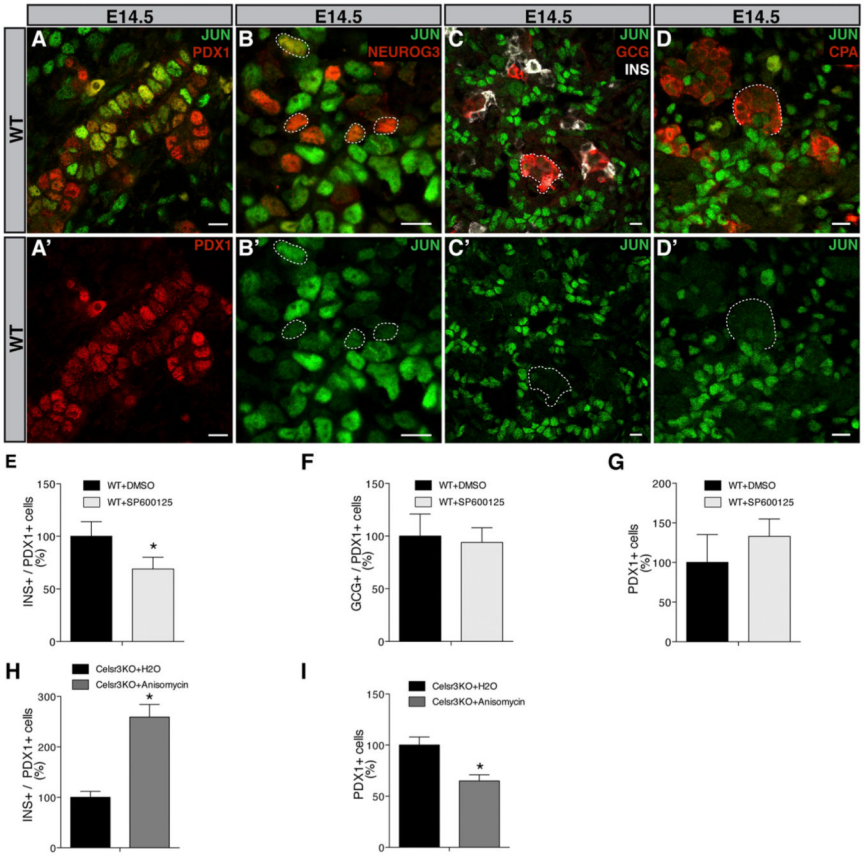

Figure 7. *Celsr2+3* Control Beta Cell Differentiation via the JNK Signaling Pathway

(A-D) E14.5 pancreas section immunostained with antibodies against PDX1, NEUROG3, INS and GCG, CPA, and Jun. (A and A′) PDX1$^+$ progenitors located in cords are JUN$^+$. (B-D′) Most of the NEUROG3$^+$ endocrine progenitors are JUN$^+$, although at a lower level than neighboring PDX1$^+$ cells, whereas INS$^+$ and CGC$^+$ cells (endocrine cells) and CPA$^+$ cells (acinar cells) are JUN$^-$. (A′) PDX1 only (red). (B′-D′) Only JUN (green). Scale bar, 10 μm.

(E-G) E12.5 WT pancreatic explants were treated with DMSO or with 5 μM SP600125, a JNK inhibitor, diluted in DMSO for 48 hr. Quantification of immunostained explants for Insulin, Glucagon, and PDX1. The number of INS$^+$/PDX1$^+$ cells is significantly decreased (n = 4), *p < 0.05.

(H and I) Rescue experiment treating E12.5 *Celsr3* KO pancreatic explants with water or with 50 ng/ml of anisomycin, a JNK agonist, diluted in water for 48 hr. Quantification of immunostained explants for Insulin and PDX1. The number of PDX1+ cells is reduced by anisomycin. The number of INS$^+$/PDX1$^+$ cells is significantly increased (n = 4), *p < 0.05. Quantifications of INS cells were normalized to PDX1 to measure a differentiation flux from progenitors in these experiments where PDX1 cell numbers were affected by one of the compounds. Although some PDX1+ cells also express Insulin, their relative number is negligible.

Bars show SDs and p values are calculated according to the Mann-Whitney U test. See also Figure S5.